

Gaussian Tone Reservation Clipping and Filtering for PAPR Mitigation

Yves Louet*, Jacques Palicot* and Désiré Guel†

*CentraleSupélec/IETR, CentraleSupélec Campus de Rennes, 35510 Cesson-Sévigné, France

{yves.louet, jacques.palicot}@centralesupelec.fr

† Nokia Networks 7 Route de Villejust, 91620 Nozay, France
desire.guel@nokia.com

Abstract—A Gaussian function for clipping associated to a Tone Reservation filtering is presented in this paper in order to decrease multicarrier Peak to Average Power Ratio (PAPR). The advantage of this approach is twofold: first, the Gaussian clipping function is a soft non-linear function which keeps constant the average power of the signal, which is a characteristic of great importance in real transmission; second, the Tone Reservation filtering by inserting the corrected signal on reserved carriers guaranties a complete downward compatibility (it means that the receiver does not need to be changed with the update of the transmitter) with classical receivers. The filtering is performed in the frequency domain by putting the corrected signal on the free carriers of the considered standard (in our case the Wifi IEEE802.11). Furthermore, our approach does not need any side information. In addition to the previous advantages, extensive simulations show very interesting performance in the complexity/PAPR decreasing trade-off compared to others similar methods.

Index Terms—PAPR; clipping; Gaussian; OFDM.

I. INTRODUCTION

Orthogonal Frequency Division Multiplexing (OFDM), although used in many standards such as 4G and 5G, IEEE 802.11a/g, IEEE 802.16, HIPERLAN/2, and Digital Video Broadcasting (DVB), is prone to high Peak-to-Average Power Ratios (PAPR). Large PAPR values require linear High Power Amplifiers (HPA), which is not energy efficient. The combination of an insufficiently linear HPA with a signal of large PAPR values leads to in and out of band distortions as explained in [1] which was the starting point of this paper.

A huge quantity of works on PAPR topic has been published for decades along two axes: find its theoretical distribution and/or propose powerful methods to mitigate its high values. The reader may find some last developments in different contexts in [2], [3], [4], [5], [6].

The simplest way to reduce PAPR is to deliberately clip and filter the OFDM signal before amplification. However, clipping is a nonlinear process and may cause significant distortions that degrade the Bit Error Rate (BER) and increase adjacent out-of-band carriers [7]. To avoid this degradation the solution we proposed in [8] consists in transforming any adding mitigation method into Tone Reservation (TR) method by an adequate frequency domain filtering. Thus, the resulting PAPR mitigation method is fully downward compatible and does not deteriorate the useful signal. The contributions of this paper which is an extension of [1] are:

- first, we propose a new clipping function, the Gaussian clipping (GC) function, which has the main advantage, compared to other clipping functions of the literature, to keep constant the average power.
- second, we transform this GC function into a TR method, thanks to the method described in [8]. The resulting Gaussian Tone Reservation Clipping and Filtering method is a fully downward compatible method, whose performance depend on the number of reserved tones. Because the filtering process is included by principle in the TR method we will refer to Tone Reservation with Gaussian Clipping Function (TR-GCF).
- third, we compute the complexity of the method and show that the TR-GCF mitigation method offers the best trade-off between PAPR reduction, average power variation and complexity.

After a recall of some basics regarding OFDM in Section II, we present in Section III the clipping functions of the literature and the proposed Gaussian clipping function is presented in Section III-D. Section IV deals with theoretical performance of the Gaussian clipping function and Section V compares its performance with other clipping functions. Section VI deals with the use of Tone Reservation method with Gaussian clipping and the associated algorithm while Section VII presents simulation results in the context of WLAN systems. Section VIII concludes the paper.

II. OFDM SYSTEMS AND PAPR ISSUE

Throughout this paper, the continuous-time baseband representation of an OFDM symbol is given by

$$x(t) = \frac{1}{\sqrt{N}} \sum_{k=0}^{N-1} X_k e^{j2\pi f_k t}, \quad 0 \leq t \leq T_s, \quad (1)$$

where N data symbols X_k form an OFDM symbol $\mathbf{X} = [X_0, \dots, X_{N-1}]^T$, $f_k = \frac{k}{T_s}$ and T_s is the time duration of the OFDM symbol.

The OFDM symbol represented by the vector $\mathbf{X} = [X_0 \dots X_{N-1}]^T$ is transformed via an Inverse Discrete Fourier Transform (IDFT) into the T_s/N -spaced discrete-time vector $\mathbf{x} = x[n] = [x_0 \dots x_{N-1}]^T$, i.e.,

$$x_n = \frac{1}{\sqrt{N}} \sum_{k=0}^{N-1} X_k e^{j2\pi \frac{n}{N} k}, \quad 0 \leq n \leq N-1. \quad (2)$$

In this paper, the discrete-time indexing $[n]$ denotes Nyquist rate samples. Since oversampling is required in practice, we will introduce the notation $x[n/L]$ to denote oversampling by a factor of L . Several oversampling strategies of $x[n/L]$ can be defined. From now on, the oversampled IDFT output will refer to an oversampled of (2), which is expressed as follows

$$x[n/L] = \frac{1}{\sqrt{N}} \sum_{k=0}^{NL-1} X_k e^{j2\pi \frac{n}{NL} k}, \quad 0 \leq n \leq NL-1. \quad (3)$$

The above expression (3) can be implemented by using an IDFT of length NL with input vector

$$\mathbf{X}^{(L)} = \left[X_0, \dots, X_{\frac{N}{2}-1}, \underbrace{0, \dots, 0}_{(L-1)N \text{ zeros}}, X_{\frac{N}{2}}, \dots, X_{N-1} \right].$$

The PAPR of the signal $x(t)$ is defined as

$$\text{PAPR}_{[x]} \triangleq \frac{\max_{t \in [0, T_s]} |x(t)|^2}{\mathcal{P}_x}, \quad (4)$$

where $\mathcal{P}_x = E\{|x(t)|^2\}$ is the average signal power and $E\{\cdot\}$ is the statistical expectation operator. Note that, in order to accurately describe the PAPR, an oversampling factor $L \geq 4$ is required. In fact, the PAPR is practically computed in the analog domain and hence, to "see" the peaks between the samples, we need to oversample the signal with regards to the symbol frequency.

In the literature, it is customary to use the Complementary Cumulative Distribution Function (CCDF) of the PAPR as a performance criterion. It is given by

$$\text{CCDF}_{[x]}(\psi) \triangleq \Pr\{\text{PAPR}_{[x]} \geq \psi\}.$$

Accordingly the PAPR reduction gain ΔPAPR is defined as the gap between PAPR before and after applying a reduction method, for a given probability level.

III. CLIPPING FUNCTIONS

In this section, we first present clipping techniques [18] and the Gaussian clipping used in the remainder of the paper. Whatever the clipping technique to reduce PAPR, the output signal y_n , in terms of the input signal x_n is given as follows:

$$y_n = f(|x_n|) e^{j\varphi_n}, \quad (5)$$

where φ_n is the x_n phase and $f(\cdot)$ is the clipping function.

A. Classical Clipping technique

The Classical Clipping proposed in [7], [20] is one of the most popular clipping technique for PAPR reduction known in the literature. It is sometimes called hard clipping and to avoid any confusion, it is called Classical Clipping (CC) in this paper. In [7], its effects on the performance of OFDM, including the power spectral density, the PAPR and BER have been evaluated. The function used for CC technique is defined below and depicted in Fig. 1(a):

$$f(r) = \begin{cases} r, & r \leq A \\ A, & r > A \end{cases}, \quad (6)$$

where A is the clipping threshold.

B. Deep Clipping technique

Deep Clipping (DC) has been proposed in [22] to solve the peaks regrowth issue due to the out-of-band filtering of the classical clipping and filtering method. In DC technique, the clipping function is modified in order to "deeply" clip the high amplitude peaks. A parameter called clipping depth factor has been introduced in order to control the depth of the clipping. The function-based clipping used for DC technique is defined below and depicted in Fig. 1(b):

$$f(r) = \begin{cases} r, & r \leq A \\ A - \beta(r - A), & A < r \leq \frac{1+\beta}{\beta}A \\ 0, & r > \frac{1+\beta}{\beta}A \end{cases},$$

where β is called the clipping depth factor.

C. Smooth Clipping technique

In [23], a Smooth Clipping (SC) technique is used to reduce the OFDM PAPR. In this paper, the function based-clipping for SC technique is defined below and depicted in Fig. 1(c).

$$f(r) = \begin{cases} r - \frac{1}{b}r^3, & r \leq \frac{3}{2}A \\ A, & r > \frac{3}{2}A \end{cases},$$

where $b = \frac{27}{4}A^2$. These three clipping functions are drawn on Fig. 1 and have been completely studied and compared in [18]. In the literature it exists other clipping function, among them we may cite the invertible clipping [24].

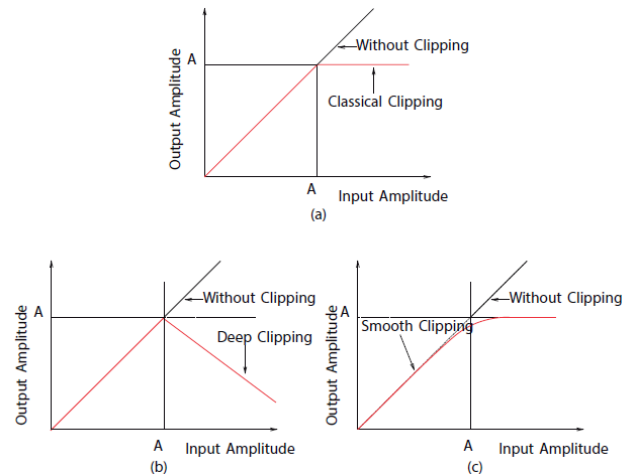


Fig. 1. Functions-based clipping for PAPR reduction

D. Gaussian Clipping technique

In this subsection, we present the Gaussian Clipping (GC) for PAPR reduction. We start from the Gaussian function, which is drawn in Fig. 2. It will operate on the multicarrier signal amplitudes in order to decrease its PAPR. In this context, only positive values are taken into account, because the signal modulus is always positive.

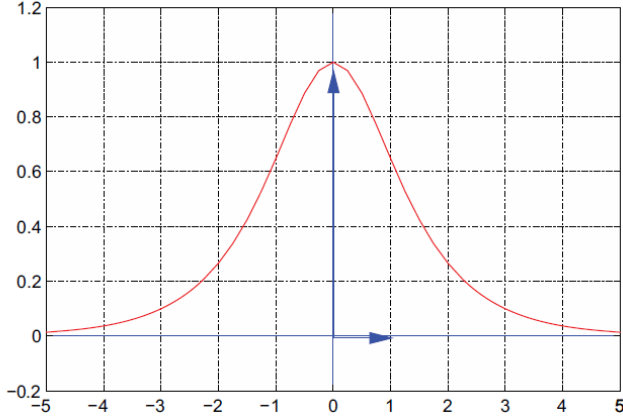


Fig. 2. Gaussian clipping function

The GC function $f(\cdot)$, associated to this Gaussian function, is expressed as:

$$f(r) = Ae^{-(\eta r)^2}, \quad r \geq 0. \quad (7)$$

The parameters A and η control the performance of the method (the transmitted mean power variation and the PAPR reduction capability).

The GC technique whose expression is given in (7) can reduce the OFDM PAPR by increasing low amplitudes samples and by decreasing high amplitudes samples, as illustrated in Fig. 3.

Fig. 3 shows that for samples r_n such that $r_n = |x_n| \leq S$, the signal is amplified whereas for samples r_n such that $r_n \geq S$ the signal is attenuated. S , which corresponds to the threshold between amplification and reduction of the signal is obtained by solving (8) and is given by (9):

$$f[r] = Ae^{-(\eta r)^2} = Ar, \quad (8)$$

what gives:

$$S = \sqrt{\frac{W(2\eta)}{2\eta}}, \quad (9)$$

where $W(\cdot)$ is the Lambert function. It has to be noted from (9) that S depends only on the η parameter of the GC (see (7)). It is therefore clear that S and consequently η , drives the PAPR reduction gain of the GC. We will now explain the influence of A on the PAPR reduction gain. We remind that one of our objectives is to keep constant the average power between the input and the output of clipping. Therefore, we would like to have $\mathcal{P}_y = \mathcal{P}_x$, where \mathcal{P}_x and \mathcal{P}_y are the average powers before and after the PAPR mitigation technique respectively. Considering (7), \mathcal{P}_y is given by (10):

$$\mathcal{P}_y = \int_0^{\infty} f(r)^2 p_x(r) dr = A^2 \int_0^{\infty} e^{-2(\eta r)^2} p_x(r) dr, \quad (10)$$

where $p_x(r)$ is the probability density function (PDF) of the considered signal envelope (here the OFDM signal).

Therefore, the ratio γ between \mathcal{P}_x and \mathcal{P}_y is expressed as follows:

$$\gamma = \frac{\mathcal{P}_y}{\mathcal{P}_x} = \frac{A^2}{\mathcal{P}_x} \int_0^{\infty} e^{-2(\eta r)^2} p_x(r) dr. \quad (11)$$

As shown by (11), A and η influence the ratio γ . This means that it is possible to tune the ratio γ thanks to parameter A without modifying the PAPR reduction gain, for a given η . In fact we showed that the PAPR reduction gain only depends on η parameter.

The A parameter value which gives $\mathcal{P}_y = \mathcal{P}_x$ is given by: (12)

$$A^{(\text{opt})} = \frac{\sqrt{\mathcal{P}_x}}{\left[\int_0^{\infty} e^{-2(\eta r)^2} p_x(r) dr \right]^{\frac{1}{2}}}. \quad (12)$$

To sum up, we have shown that η drives the PAPR reduction gain whereas A drives the average power variation for a given η .

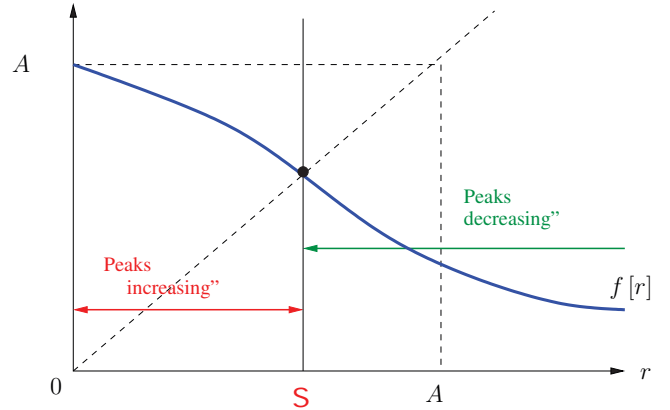


Fig. 3. Attenuation and amplification with GC function

IV. THEORETICAL STUDY OF GAUSSIAN CLIPPING

In this section, we analyze theoretically the behavior of the GC function. We first focus on the average power variation $\Delta E = 10 \log_{10}(\gamma)$. Then, we study the PAPR CCDF at the output of the GC function. We are interested in the PAPR reduction gain ΔPAPR for a CCDF value of 10^{-2} before and after clipping.

A. Average power variation analysis

As mentioned previously $p_x(r)$ is PDF of the OFDM envelope and can be assimilated to a Rayleigh distribution for a large number of OFDM subcarriers. Its expression is given by:

$$p_x(r) = \frac{2r}{P_x} e^{-\frac{r^2}{P_x}}, \quad r \geq 0. \quad (13)$$

Then, the expression of the transmitted mean power \mathcal{P}_y is

$$\mathcal{P}_y = \int_0^{+\infty} \left[A e^{-(\eta r)^2} \right]^2 \frac{2r}{P_x} e^{-\frac{r^2}{P_x}} = \frac{A^2}{1 + 2\eta^2 \mathcal{P}_x}. \quad (14)$$

As a result,

$$\gamma \triangleq \frac{\mathcal{P}_y}{\mathcal{P}_x} = \frac{A^2}{(1 + 2\eta^2 \mathcal{P}_x) \mathcal{P}_x}. \quad (15)$$

From (15), it is easy to compute the value of $A^{(\text{opt})}$ (for $\mathcal{P}_y = \mathcal{P}_x$) which is expressed as:

$$A^{(\text{opt})} = \left[(1 + 2\eta^2 \mathcal{P}_x) \mathcal{P}_x \right]^{\frac{1}{2}}. \quad (16)$$

It is interesting to note that $A^{(\text{opt})}$ depends on η (which controls the PAPR reduction gain) and the average power of input signal.

The average power variations related to the GC are compared to simulation results in Fig. 4. Results show a good match between theory (15) and simulations. For a given η value, the average power is a linear function of A . Therefore, for a given η parameter value, it is possible to find the value of $A^{(\text{opt})}$ which keeps constant the average power. This is given by $\gamma = 0$.

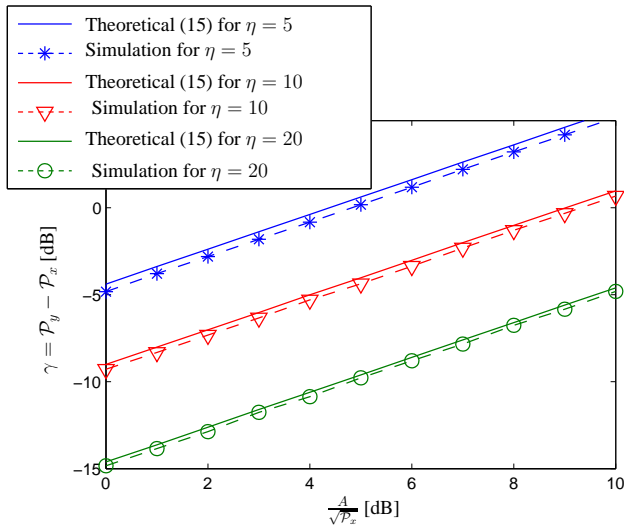


Fig. 4. Average power variations for several values of $\frac{A}{\sqrt{P_x}}$

B. PAPR distribution analysis

In this subsection, the PAPR CCDF is derived analytically. To perform this analysis, like in [9] for the classical OFDM PAPR, we assume that the signals $x(t)$ and $y(t)$ (input and output of the GC respectively) are sampled at the Nyquist rate

(that means with an oversampling factor $L = 1$). Therefore, input and output samples x_n and y_n are respectively given by:

$$\begin{aligned} x_n &= x \left(\frac{n}{N} T_s \right), \\ y_n &= y \left(\frac{n}{N} T_s \right), \end{aligned} \quad (17)$$

where $0 \leq n < N$. The signals x_n and y_n may also be written as:

$$\begin{aligned} x_n &= r_n e^{j\phi_n}, \\ y_n &= f[r_n] e^{j\phi_n} = v_n e^{j\phi_n}, \end{aligned} \quad (18)$$

where r_n is the amplitude of x_n et ϕ_n its phase; $v_n = f(r_n)$ is the amplitude of y_n . The PAPR of y_n is given by :

$$\text{PAPR}_{[y]} = \frac{\max_{0 \leq n < N} |y_n|^2}{\mathcal{P}_y} = \frac{\max_{0 \leq n < N} v_n^2}{\mathcal{P}_y}. \quad (19)$$

By applying the same development as in [9], and by assuming independence between v_n values we get:

$$\begin{aligned} \text{CCDF}_{[y]}(\tilde{\psi}) &= \Pr \left[\text{PAPR}_{[y]} \geq \tilde{\psi} \right] = \Pr \left[\frac{\max_n v_n^2}{\mathcal{P}_y} \geq \tilde{\psi} \right] \\ &\simeq 1 - \prod_{n=0}^{N-1} \left\{ \Pr \left[\frac{f(r_n)^2}{\mathcal{P}_y} \leq \tilde{\psi} \right] \right\}, \\ &\simeq 1 - \prod_{n=0}^{N-1} \left\{ \Pr \left[f(r_n) \leq \sqrt{\tilde{\psi} \mathcal{P}_y} \right] \right\} \end{aligned} \quad (20)$$

where $f[r]$ is the GC function given by (7).

Then,

$$\text{CCDF}_{[y]}(\tilde{\psi}) \simeq 1 - \prod_{n=0}^{N-1} \left\{ \Pr \left[r_n \geq \frac{1}{\eta} \left[\ln \left(\frac{A}{\sqrt{\tilde{\psi} \mathcal{P}_y}} \right) \right]^{\frac{1}{2}} \right] \right\}. \quad (21)$$

As r_n follows a Rayleigh i.i.d random process whose PDF is given by (13), (21) becomes:

$$\begin{aligned} \text{CCDF}_{[y]}(\tilde{\psi}) &\simeq 1 - \prod_{n=0}^{N-1} \left[e^{-\frac{\ln \left(\frac{A}{\sqrt{\tilde{\psi} \mathcal{P}_y}} \right)}{\eta^2 \mathcal{P}_x}} \right], \\ &\simeq 1 - e^{-N \frac{\ln \left(\frac{A}{\sqrt{\tilde{\psi} \mathcal{P}_y}} \right)}{\eta^2 \mathcal{P}_x}}. \end{aligned} \quad (22)$$

The PAPR reduction gain is compared to simulation results and is presented in Fig. 5 for several values of η . It shows that the theoretical approximation of (22) is very close to simulation results.

The PAPR reduction gain decreases when η increases. This result provides an upper bound of η . In fact it should be smaller than 8 to have a positive PAPR reduction gain what is the objective.

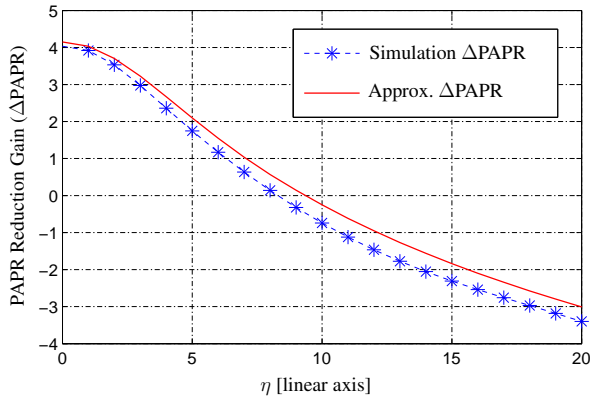


Fig. 5. PAPR reduction gain comparison between theoretical and simulation results versus η parameter for $\frac{A}{\sqrt{P_x}} = 3$ dB

V. COMPARATIVE STUDY WITH OTHER CLIPPING FUNCTIONS

In this subsection, GC performance are compared to classical clipping (Section III-A), Deep clipping (Section III-B) and Smooth clipping (Section III-C) performance. Although these three baseline algorithms are not recent, they are most of the time considered for PAPR reduction (especially hard and smooth clipping) and associated with filtering. This is the reason why we took these three approaches as a comparison basis.

This comparative study is performed in the context of the WLAN standard IEEE 802.11 a/g, whose parameters are given in Table I.

TABLE I
SIMULATION PARAMETERS

| System parameters | Values |
|--------------------------|----------|
| Modulation type | 16-QAM |
| Carriers number | $N = 64$ |
| Data sub carriers number | 48 |
| Pilots number | 4 |
| Oversampling factor | $L = 4$ |
| Channel type | AWGN |

In Fig. 6 the PAPR reduction gain, ΔPAPR , is analyzed for the four clipping techniques in function of the average power variation ΔE . For the Classical, Deep and Smooth clipping functions, ΔPAPR decreases with ΔE and becomes very small for $\Delta E \simeq 0$ dB. At the opposite, ΔPAPR with the GC is quasi constant with ΔE . In fact, whatever the value of ΔE , ΔPAPR of GC equals 5.2 dB. This result is the great advantage of the GC, because it offers a PAPR reduction gain of 5.2 dB without modifying the average power. To reach this result it is necessary to set $\frac{A}{\sqrt{P_x}}$ to 0.45 dB as shown in Fig. 7.

In this figure, the influence of the parameter A is presented. The results show A controls the average power variation without modifying the PAPR reduction gain. This result is very important. In fact, it is possible to choose A in such a way that $\mathcal{P}_y = \mathcal{P}_x$ without modifying the PAPR reduction

gain. In other words, with the GC function it is possible to reach a PAPR reduction gain of 5 dB with an average power variation $\Delta E = 0$.

Fig. 8 presents the BER performance. As expected, these techniques degrade the BER. In fact the signal resulting from clipping functions is useful for PAPR reduction but behaves also as an interferer which deteriorates the signal both in and out of band. Generally out of band degradation can be removed by filtering (it is why clipping techniques are generally named clipping and filtering techniques). GC is the one which degrades the most the BER. This was expected because the PAPR reduction was the highest. That means that GC (as every clipping function) could not be used without BER improvement. To mitigate the BER degradation due to clipping noise (whatever the clipping function), several techniques could be performed:

- by inverting the clipping function or by iterative subtraction of the noise regenerated by the clipping function at the receiver [10]. Iterative methods to subtract the estimated noise have been proposed in [11] and [12]. The main drawbacks, in our point of view, are (i) these techniques become no more downward compatible and (ii) the complexity is high at the receiver side. Furthermore, the out of band noise will degrade the signal in the adjacent band (the so called shoulders), which is, of course, not acceptable.
- another alternative consists in turning the clipping method into a Tone Reservation (TR) method. By principle TR does not deteriorated the BER. This technique has several advantages: (i) it is performed at the transmitter side, (ii) it is downward compatible and (iii) it is very simple to set up. This approach is detailed in the following section.

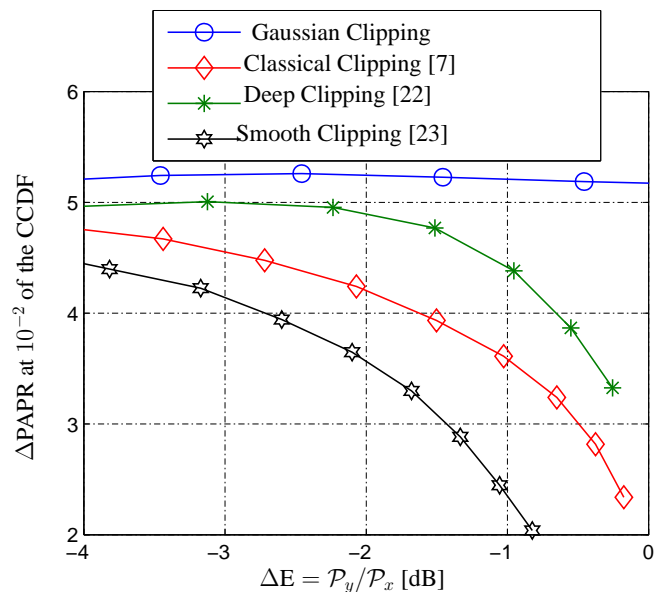


Fig. 6. PAPR reduction gain versus the added power

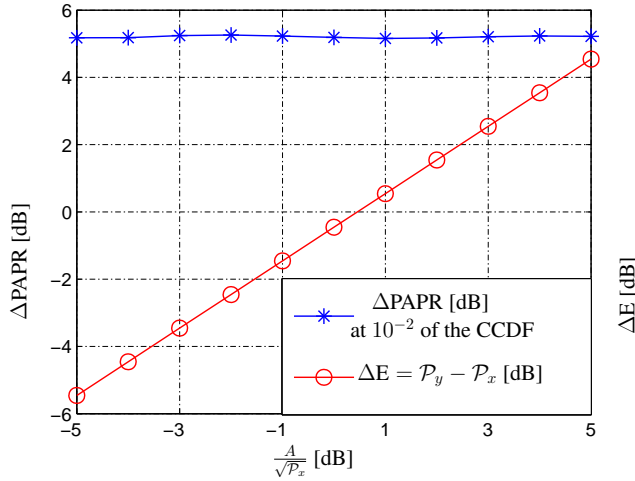


Fig. 7. PAPR reduction gain and average power variation of the GC function versus A parameter

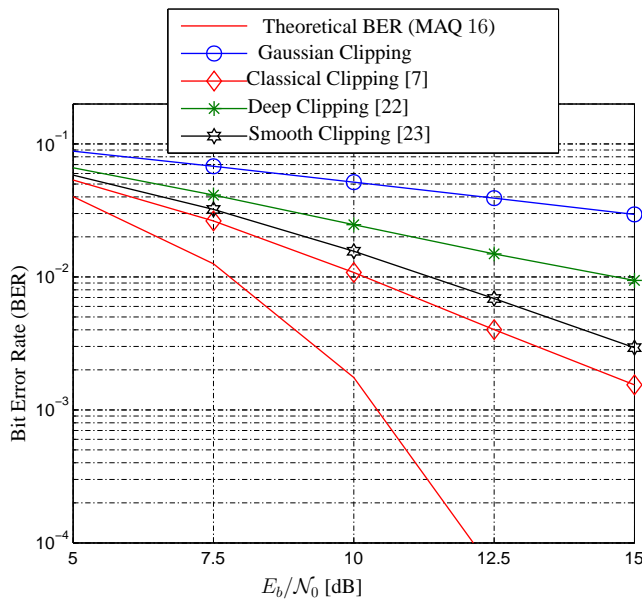


Fig. 8. BER comparison for the clipping functions

VI. TONE RESERVATION BASED GAUSSIAN CLIPPING

A. Context of Tone Reservation

We are focusing here on one of the most common methods called Tone Reservation (TR) [14], because it is able to decrease the PAPR without degrading the BER. This method has been standardized in DVB-T2. It consists in computing a corrective signal (also, called peak-reducing signal) which is inserted on a set of reserved tones. It is added to the original signal, leading to a PAPR reduction of the latter. The simplest way to generate and compute the corrective signal is to deliberately clip the OFDM signal [13]. In this paper we propose to use the GC function presented previously. This function keeps constant the average power of the signal which is of great importance in practice. Then, we insert this corrective signal on the reserved tones by a suitable frequency domain filtering, as described in [8]. Thus, the resulting PAPR

reduction method is a fully downward compatible method which does not degrade the useful signal.

B. Tone Reservation principle

The TR technique [14], [15] is an adding signal technique. It has been studied mainly for the OFDM signal, without any specification of a standard.

The idea of the TR technique is to reserve N_r sub-carriers (also called tones) in the OFDM symbol on which an appropriate information will be added in order to change the time signal, so as to reduce its dynamics. In this technique, the transmitter and the receiver agree on the number and the positions of the subcarriers which are reserved to carry the corrective signal to decrease the PAPR.

In this paper, the TR technique will be implemented using the “unused subcarriers”, so-called “null subcarriers”, that are considered in the standards in order to make the technique downward compatible. The diagram of the method is given in Fig. 9.

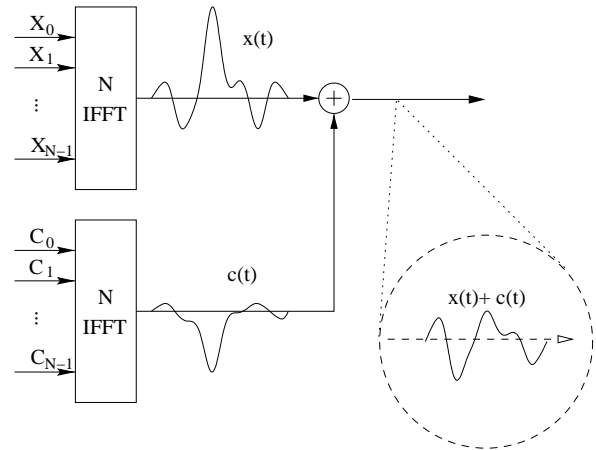


Fig. 9. Illustration of the Tone Reservation method

The peak-reducing signal c_n is carried by the reserved sub-carriers and the peak-reduced signal is given by

$$y_n = x_n + c_n = \frac{1}{\sqrt{N}} \sum_{k=0}^{NL-1} (X_k + C_k) e^{2j\pi \frac{kn}{NL}}, \quad (23)$$

where $0 \leq n \leq NL - 1$ and $\mathbf{C} = [C_0, \dots, C_{NL-1}]$ is the set of peak-reducing subcarriers.

To set up a new TR technique, two problems have to be tackled by first generating an adding signal c_n and, second, inserting it on the reserved carriers. Of course, it is possible to jointly solve these two problems. In the next subsection, we will present a possible way to generate this signal using a clipping function and a way to insert the adding signal on the reserved tones thanks to a frequency domain filtering.

C. Signal adding principle

In the signal adding context, the PAPR is reduced by adding a corrective signal sometimes called “peak reducing signal”

or “peak canceling signal” [8]. A block diagram of the OFDM transmitter with an adding signal technique for PAPR reduction is shown in Fig. 10.

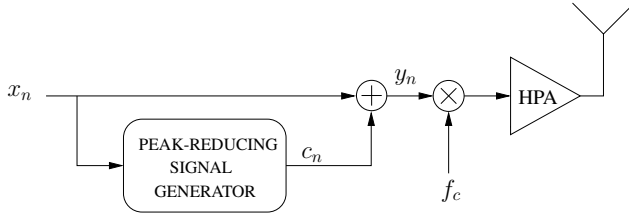


Fig. 10. Tone Reservation as an adding signal method

The peak-reducing signal c_n is computed according to PAPR reduction techniques. In [15], c_n is computed based on Second Order Cone Program (SOCP) in the frequency domain, while in [26], c_n is computed in the frequency domain with the Gradient algorithm, which is a low-complexity algorithm. In [13], the peak-reducing signal c_n is computed in the time domain based on a nonlinear function $f(\cdot)$ called “function for PAPR reduction”. Using $f(\cdot)$ to reduce the PAPR of x_n , the peak reducing signal c_n is written as

$$c_n = f[|x_n|] e^{j\varphi_n} - x_n, \quad (24)$$

where φ_n is the phase of x_n . In this paper, we use this simple way to compute the desired peak-reducing signal, where $f(\cdot)$ is the GC function.

D. Tone Reservation Filtering

Let \tilde{c}_n be the signal at the output of the FFT/IFFT block, as shown in Fig. 11.

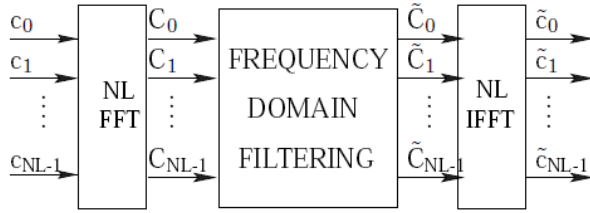


Fig. 11. Digital filtering-based FFT/IFFT

The FFT/IFFT consists of a FFT followed by an IFFT. The forward FFT transforms c_n to the frequency-domain. The discrete frequency components of c_n on the reserved subcarriers are passed unchanged, while the data subcarriers and the Out Of Band (OOB) components are set to zero. The relationship between the input and the output of the FFT/IFFT filter is given by:

$$\tilde{c}_n = \mathcal{F}^{-1}(\mathcal{H}[\mathcal{F}(c_n)]), \quad (25)$$

where \mathcal{F} represents the FFT function, \mathcal{F}^{-1} is the IFFT function and \mathcal{H} is the digital filter response in the frequency domain. The FFT/IFFT filter complexity is approximated as $\mathcal{O}(NL \log_2 NL)$. The principle of FFT/IFFT filter with a TR technique is shown in Fig. 12.

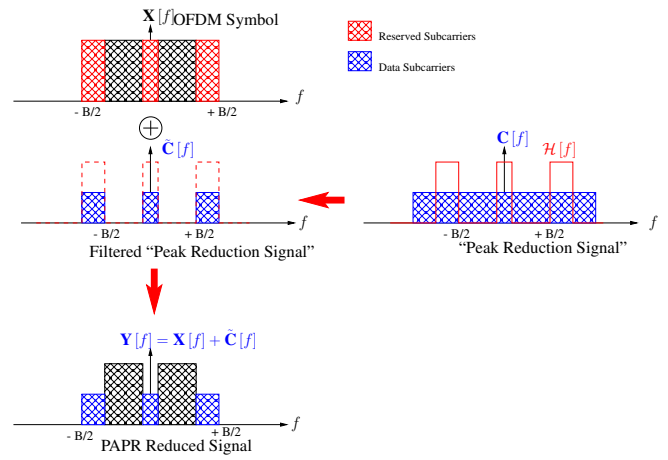


Fig. 12. FFT/IFFT filter based on TR

E. Associated iterative algorithm

In this section, we detail the algorithm explained previously with an iterative principle as presented in [8]. This algorithm is illustrated in Fig. 13. We can easily distinguish two sub-blocks within the TR-GCF technique: the PAPR reduction signal generator based on the Gaussian function and the digital filtering based on FFT/IFFT operations.

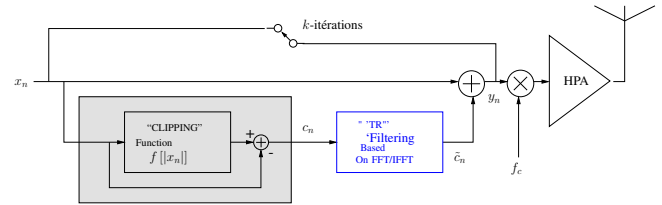


Fig. 13. Diagram of TR-GCF method

In order to reduce the PAPR as much as possible, the algorithm is based on an iterative procedure whose principle is as follows:

- Set up the locations of the reserved subcarriers \mathcal{R} and the maximum iteration number N_{iter} , and choose the function for PAPR reduction $f(\cdot)$.
- Set up $i = 0$, where $x_n^{(0)} = x_n$ is the time-domain OFDM signal.
- Compute the (i) -iteration PAPR reduction signal as:

$$\tilde{c}_n^{(i)} = f_{\Delta} \left[f \left(x_n^{(i)} \right) - x_n^{(i)} \right], \quad (26)$$

where $f_{\Delta} = \mathcal{F}^{-1} \circ \mathcal{H} \circ \mathcal{F}$ is the FFT/IFFT based digital filter response in time domain.

- Compute the $(i + 1)$ -iteration PAPR reduced signal as:

$$x_n^{(i+1)} = x_n^{(i)} + \beta_{opt}^{(i)} \tilde{c}_n^{(i)}. \quad (27)$$

The scaling factor $\beta_{opt}^{(i)}$ is the solution of the following optimization problem:

$$\beta_{opt}^{(i)} = \arg \min_{\beta} \left[\max_n \left| x_n^{(i)} + \beta \tilde{c}_n^{(i)} \right| \right]. \quad (28)$$

An exact solution of (28) exists but leads to a high computation complexity. In [27] it is shown that a suboptimal solution of (28) is given by minimizing the total power of the samples with $|x_n^{(i)} + \tilde{c}_n^{(i)}| > A$, where A is a magnitude threshold. Solving (28) leads to

$$\beta_{opt}^{(i)} = -\frac{\sum_{n \in \mathcal{S}_p^{(i)}} x_n^{(i)} \tilde{c}_n^{*(i)}}{\sum_{n \in \mathcal{S}_p^{(i)}} |c_n^{(i)}|^2}, \quad (29)$$

where $(\cdot)^*$ is the mathematical conjugate function, and where, $\mathcal{S}_p^{(i)} = \{n : |x_n^{(i)} + \tilde{c}_n^{(i)}| > A\}$.

The complexity of calculating $\beta_{opt}^{(i)}$ is $\mathcal{O}(\mathcal{N}_p)$, where \mathcal{N}_p is the size of $\mathcal{S}_p^{(i)}$. After \mathcal{N}_{iter} iterations, the TR-GCF algorithm complexity can be approximated to $\mathcal{N}_{iter} [\mathcal{O}(NL \log_2 NL) + \mathcal{O}(\mathcal{N}_p)] \simeq \mathcal{O}(\mathcal{N}_{iter} NL \log_2 NL)$. It is worth noting that the system complexity grows linearly with the number of iterations.

VII. APPLICATION TO WLAN SYSTEMS

In the WLAN IEEE 802.11a/g standard, IFFT length N equals 64. Out of these 64 subcarriers, 48 subcarriers are used for data, while 4 subcarriers are used for pilots. The remaining 12 subcarriers are unused (null) subcarriers located at the positions $\mathcal{R} = \{0, 27, \dots, 37\}$ of the IFFT input.

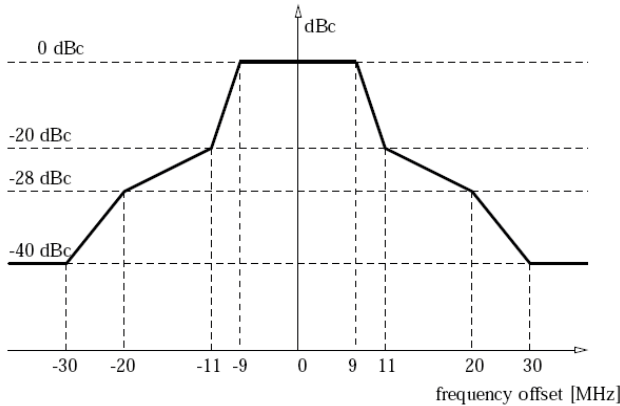


Fig. 14. Spectral power mask of WLAN

The IEEE 802.11a/g standard specifications are given in [28] and the transmit spectral mask requirements are shown in Fig. 14.

A. TR-GCF technique performance

In this section, we simulate the performance of the TR-GCF (influence of η and \mathcal{N}_{iter} on the PAPR reduction and the Power Spectral Density) in a WLAN (IEEE 802.11 a/g) context. Fig. 15 shows the influence of parameter η on the PAPR reduction gain Δ PAPR. For $\eta = 6$, the maximum PAPR reduction gain is achieved. In the rest of our simulations, η will be set to 6 in order to reach the maximum of PAPR reduction.

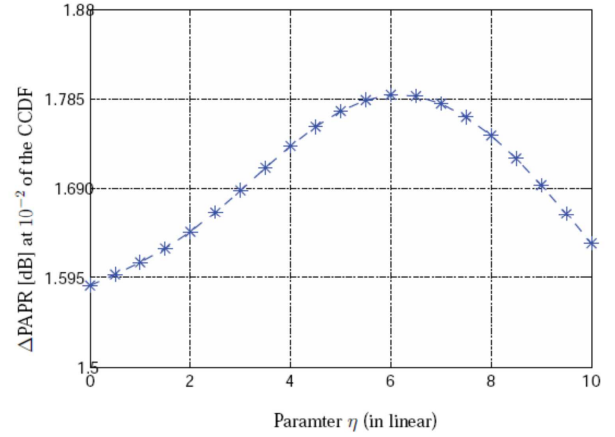


Fig. 15. PAPR reduction performance of TR-GCF technique versus η for $\mathcal{N}_{iter} = 5$

Fig. 16 shows the performance of PAPR reduction for different iteration numbers. As expected, the PAPR reduction gain increases with the number of iterations \mathcal{N}_{iter} . For example, at 10^{-2} of the CCDF, Δ PAPR is about 1.10 dB, 1.65 dB, 1.77 dB and 1.80 dB for $\mathcal{N}_{iter} = 1, 3, 5$ and 10, respectively. However, the PAPR reduction gain converges from $\mathcal{N}_{iter} \geq 5$ because, in Fig. 16, there is no significant reduction of PAPR between $\mathcal{N}_{iter} = 5$ and $\mathcal{N}_{iter} = 10$.

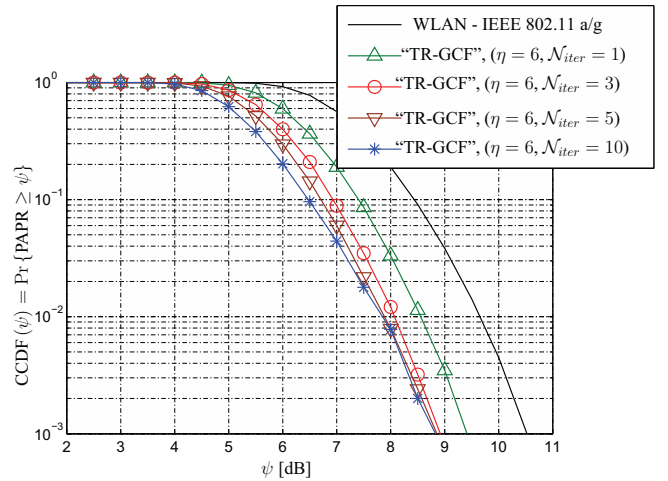


Fig. 16. TR-GCF technique PAPR reduction performance for \mathcal{N}_{iter} iterations

Fig. 17 presents the spectrum of WLAN signals before and after applying the TR-GCF technique. It shows that whatever the \mathcal{N}_{iter} value, the signal spectrum, after PAPR reduction, meets the specifications of the WLAN standard transmission. The power of the subcarriers (the unused ones which carried out the Peak reducing signal) increases with \mathcal{N}_{iter} because the power of the PAPR reduction signal increases with \mathcal{N}_{iter} . As the PAPR reduction signal is carried by the unused subcarriers (which are located besides the useful data of the IEEE 802.1a/g standard), the power level of these subcarriers increases as seen in Fig. 17. But the level of these carriers remains below the WLAN spectral mask.

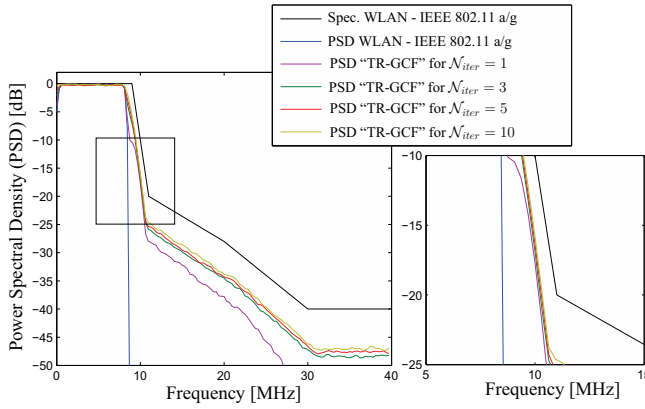


Fig. 17. WLAN signals spectrum before and after TR-GCF PAPR technique

In Fig. 18, we verify that the Bit Error Rate (BER) of the WLAN system after applying the TR-GCF technique matches the theoretical BER. We can remark that, as expected, whatever N_{iter} value, the WLAN BER matches with the theoretical BER, because all of the tones used for TR are outside of the useful band so do not interfere with the data.

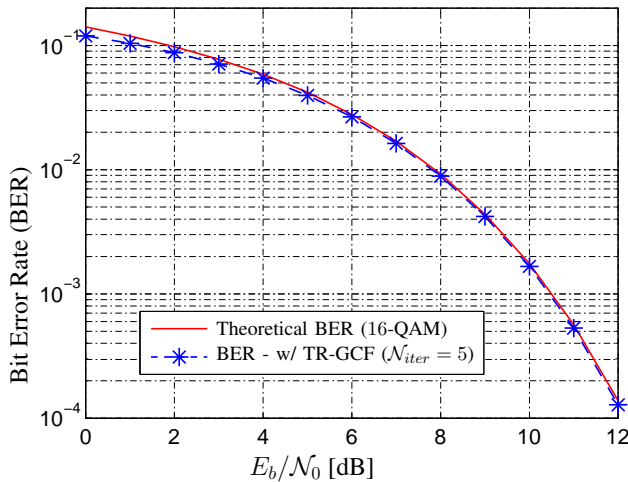


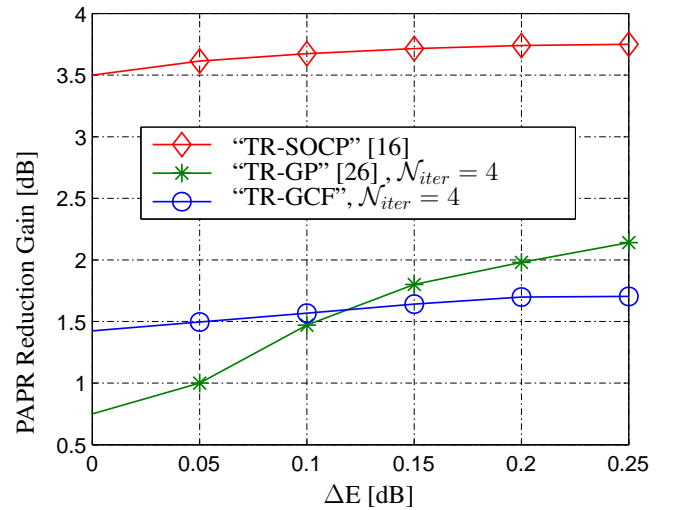
Fig. 18. WLAN BER with and without TR-GCF technique

B. Comparative study of TR-GCF with TR-GP and TR-SOCP

In this section, we compare the performance of the TR-GCF technique, which proposed in this paper, with those of the TR-GP and TR-SOCP techniques in a WLAN context. The TR techniques for PAPR reduction TR-SOCP and TR-GP are deeply described in [16] and [26] respectively.

Fig. 19 compares the reduction in PAPR of the TR-GCF, TR-GP and TR-SOCP techniques according to the variation of the average power. It shows that, in terms of PAPR reduction, the TR-SOCP is better (~ 2 dB and ~ 3 dB of PAPR reduction more than the TR-GP and TR-GCF techniques, respectively). This result is explained by the fact that TR-SOCP is an optimal TR technique in contrast to TR-GP and TR-GCF techniques which are sub-optimal TR techniques.

The major drawback of TR-SOCP technique lies in its complexity (estimated to $\mathcal{O}(N^2 N_{\mathcal{R}} L)$, where N is the number of

Fig. 19. PAPR reduction performance according to ΔE for TR-GCF, TR-GP and TR-SOCP techniques

subcarriers of the OFDM system, $N_{\mathcal{R}}$ is the number of unused sub-carriers and L is the over-sampling rate).

For small increases of the average power ($\Delta E \leq 0.1$ dB) and for the same value of N_{iter} (this means, for the same computational complexity), the TR-GCF is more efficient than TR-GP. Because we are seeking for techniques that reduce the PAPR with $\Delta E \simeq 0$ dB, then TR-GCF is interesting because of its computational complexity (compared to TR-SOCP) and in addition, its PAPR reduction gain is a quasi-constant function of the average power variation. Even if the main advantage of keeping constant the average power of the GC function is partly lost due to the frequency domain filtering of the TR method, as A controls the average power variation without affecting the PAPR reduction gain, we can choose, for a fixed value N_{iter} , the value of A which gives the lowest variation, i.e. $A^{(opt)} = \arg \min_A \Delta E$. This constraint is included in the algorithm.

The computational complexity figures given below show that under the simulation conditions of Fig. 19, TR-SOCP is by far the most complex one. It is 24 times more complex than the TR-GP and TR-GCF techniques.

TABLE II
COMPUTATIONAL COMPLEXITY

| TR-GCF | TR-GP [26] | TR-SOCP [16] |
|---|--|--------------------------------------|
| Computational complexity | | |
| $\mathcal{O}(N_{iter} N L \log_2 N L)$ | $\mathcal{O}(N_{iter} N L \log_2 N L)$ | $\mathcal{O}(N^2 N_{\mathcal{R}} L)$ |
| Comparison of the Computational complexity in the conditions of simulation of Fig. 19 | | |
| $\mathcal{O}(4 \times 2^{11})$ | $\mathcal{O}(4 \times 2^{11})$ | $\mathcal{O}(96 \times 2^{11})$ |

NL : IFFT size=256; $N_{\mathcal{R}} = 12$ is the number of reserved sub-carriers and N_{iter} the number of iterations.

VIII. CONCLUSION

Tone Reservation based Gaussian Clipping has been proposed in this paper. This new method has been obtained thanks to

a TR transformation of the adding signal resulting in the GC function. Even if the main advantage of keeping constant the average power of the GC function is partly lost due to the frequency domain filtering of the TR method, it is possible to control efficiently this average power variation ΔE . In fact as A controls the average power variation without affecting the PAPR reduction gain a simple constraint in the algorithm could control ΔE .

Performance of the TR-GCF have been evaluated through simulations and compared to other signal adding techniques. The main conclusion is that the TR-GCF technique is the best compromise between complexity and performance for downward compatible techniques.

IX. ACKNOWLEDGMENT

This work was supported by the framework of the WONG5 Project, through the French National Research Agency (ANR) under Grant ANR-15-CE25-0005.

This publication was supported by the European Union through the European Regional Development Fund (ERDF), and by the french region of Brittany, Ministry of Higher Education and Research, Rennes Metropole and Conseil Departemental 35, through the CPER Project SOPHIE / STIC-Ondes

REFERENCES

- [1] D. Guel, J. Palicot, and Y. Louet, *A New Clipping Function for PAPR Mitigation: The Gaussian Clipping Function*, Fourteenth Advanced International Conference on Telecommunications, AICT 2018, July 2018, Barcelona, Spain.
- [2] F. Sandoval, G. Poitou, and F. Gagon *Hybrid Peak-to-Average Power Ratio Reduction Techniques; Review and Performance Comparison*, IEEE Access, vol.5, pp. 27145-27161, 2017.
- [3] P. Kryszkiewicz *Amplifier-Coupled Tone Reservation for Minimization of OFDM Nonlinear Distortion*, IEEE Transactions on Vehicular Technology, vol.67, pp. 4316-4324, 2018.
- [4] S. Lin, Y. Chen, and S. Tseng *Iterative smoothing filtering schemes by using clipping noise-assisted signals for PAPR reduction in OFDM-based carrier aggregation systems*, IET Communications, vol.13, pp. 802-808, 2019.
- [5] Z. He, L. Zhou, and X. Ling *Low-Complexity PTS Scheme for PAPR Reduction in FBMC-OQAM Systems*, IEEE Communications Letters, vol.22, pp. 2322-2325, 2018.
- [6] Y. Jawhar et al. *A Review of Partial Transmit Sequence for PAPR Reduction in the OFDM Systems*, IEEE Access, vol.7, pp. 18021-18041, 2019.
- [7] X. Li and J.L.J. Cimini, *Effects of clipping and filtering on the performance of OFDM*, IEEE Communication Letters, vol. 2, pp. 131-133, May 1998.
- [8] D. Guel and J. Palicot, *Transformation of any Adding Signal Technique in Tone Reservation Technique for PAPR Mitigation thanks to Frequency Domain Filtering*, International Journal on Advances in Telecommunications, vol 4 no 1-2, 2011.
- [9] H. Ochiai and H. Imai, *On the distribution of the peak-to-average power ratio in OFDM signals*, IEEE Trans. Commun., vol. 49, pp. 282-289, Feb 2001.
- [10] R. Déjardin, M. Colas, and G. Gelle, *Comparison of iterative receivers mitigating the clipping noise of OFDM based systems*, in European Wireless Proceedings, 2007.
- [11] R. Déjardin, M. Colas, and G. Gelle, *On the iterative mitigation of clipping noise for COFDM transmissions*, European Trans. on Telecommunications, pp. 247-252, 1998.
- [12] H. Chen and A.M. Haimovich, *Iterative estimation and cancellation of clipping noise for OFDM signals*, IEEE Communications Letters, vol. 7, pp. 305-307, July 2003.
- [13] D. Guel and J. Palicot, *Clipping formulated as an adding signal technique for OFDM Peak Power Reduction*, in Proc. 69th Vehicular Technology Conference: VTC2009-Spring, 26-29 April 2009. Barcelona, Spain.
- [14] J. Tellado-Mourelo, *Peak to Average Power Reduction for Multicarrier Modulation*. Ph.D, Stanford University, Sept 1999.
- [15] S. Zabré, J. Palicot, Y. Louet, and C. Lereau, *SOCP Approach for OFDM Peak-to-Average Power Ratio Reduction in the Signal Adding Context*, in Proc. IEEE International Symposium on Signal Processing and Information Technology, pp. 834-839, 2006.
- [16] S. Zabre, *Amplification non-linéaire d'un multiplex de porteuses modulées à fort facteur de crête*, PhD thesis, University of Rennes 1, April 2007.
- [17] S. Janaaththan, C. Kasparis, and B. G. Evans, *A Gradient Based Algorithm for PAPR Reduction of OFDM using Tone Reservation Technique*, in Proc. IEEE Vehicular Technology Conference VTC Spring 2008, pp. 2977-2980, 11-14 May 2008.
- [18] D. Guel and J. Palicot, *Analysis and Comparison of Clipping techniques for OFDM Peak-to-Average Power Ratio Reduction*, in International Conference on DSP, July 2009.
- [19] J. Bussgang, *Crosscorrelation function of amplitude-distorted Gaussian signals*, Tech. Rep. 216, Research laboratory of electronics, Massachusetts Institute of Technology, Cambridge, 1952. Technical Report.
- [20] J. Armstrong, *Peak-to-average power reduction for OFDM by repeated clipping and frequency domain filtering*, Electronics Letters, vol. 38, pp. 246-247, 28 Feb. 2002.
- [21] Q. Hua, R. Raich, and G. Zhou, *On the benefits of deliberately introduced baseband nonlinearities in communication systems*, International Conference on Acoustics, Speech, and Signal Processing (ICASSP '04), vol. 2, pp. 905-908, May 2004.
- [22] S. Kimura, T. Nakamura, M. Saito, and M. Okada, *PAR reduction for OFDM signals based on deep Clipping*, 3rd International Symposium on Communications, Control and Signal Processing, vol. 2, pp. 911-916, March 2008.
- [23] P. Boonsriuang, E. Puttawong, H. Kobayashi, and T. Paungma, *PAPR Reduction Using Smooth Clipping in OFDM System*, The 3rd Information and Computer Engineering Postgraduate Workshop 2003 (ICEP'2003), vol. 2, pp. 158-161, January 2003.
- [24] S. Ragusa, J. Palicot, Y. Louet, and C. Lereau, *Invertible Clipping for Increasing the Power Efficiency of OFDM Amplification*, in IEEE International Conference on Telecommunications, May 2006.
- [25] D. Guel, J. Palicot, and Y. Louet, *Tone reservation technique based on geometric method for orthogonal frequency division multiplexing peak-to-average power ratio reduction*, IET Commun., November 2010 Volume 4, Issue 17, pp. 2065-2073.
- [26] S. Litsyn, *Peak Power Control in Multicarrier Communications*, in Cambridge University Press, 2007.
- [27] L. Wang and C. Tellambura, *An Adaptive-Scaling Algorithm for OFDM PAR Reduction Using Active Constellation Extension*, in IEEE 64th VTC-2006 Fall Vehicular Technology Conference, pp. 1-5, 25-28 Sept. 2006.
- [28] *Wireless LAN Medium Access Control (MAC) and Physical Layer (PHY) specifications*, 2000.